

## Metal Ion-Coupled Electron Transfer of a Nonheme Oxoiron(IV) Complex: Remarkable Enhancement of Electron-Transfer Rates by Sc<sup>3+</sup>

Yuma Morimoto,<sup>†</sup> Hiroaki Kotani,<sup>†</sup> Jiyun Park,<sup>‡</sup> Yong-Min Lee,<sup>‡</sup> Wonwoo Nam,<sup>\*,‡</sup> and Shunichi Fukuzumi<sup>\*,†,‡</sup>

Department of Material and Life Science, Graduate School of Engineering, Osaka University, Suita, Osaka 565-0871, Japan, and Department of Bioinspired Science, Ewha Womans University, Seoul 120-750, Korea

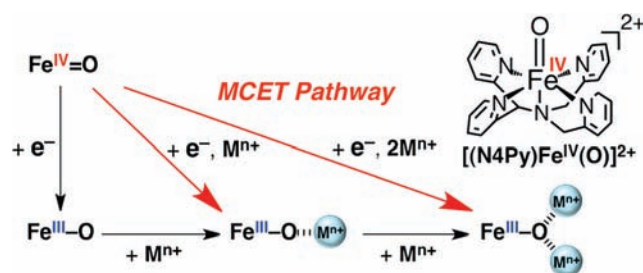
Received October 8, 2010; E-mail: wwnam@ewha.ac.kr; fukuzumi@chem.eng.osaka-u.ac.jp

**Abstract:** Rates of electron transfer from a series of one-electron reductants to a nonheme oxoiron(IV) complex, [(N4Py)Fe<sup>IV</sup>(O)]<sup>2+</sup>, are enhanced as much as 10<sup>8</sup>-fold by addition of metal ions such as Sc<sup>3+</sup>, Zn<sup>2+</sup>, Mg<sup>2+</sup>, and Ca<sup>2+</sup>; the metal ion effect follows the Lewis acidity of metal ions. The one-electron reduction potential of [(N4Py)Fe<sup>IV</sup>(O)]<sup>2+</sup> is shifted to a positive direction by 0.84 V in the presence of Sc<sup>3+</sup> ion (0.20 M).

Electron transfer (ET) is one of the most important elementary steps in biological redox processes, in which high-valent metal-oxo species are often involved as reactive species, e.g., Mn<sup>V</sup>-oxo species in water oxidation at the oxygen-evolving center (OEC) in photosystem II (PSII), Fe<sup>IV</sup>-oxo species in cytochrome *c* oxidase and P450, and nonheme iron enzymes.<sup>1–4</sup> In the OEC, Ca<sup>2+</sup> acts as an essential cofactor in the manganese-calcium (Mn<sub>4</sub>Ca) active site responsible for water oxidation in PSII, although the exact functional role of Ca<sup>2+</sup> has yet to be clarified.<sup>1</sup> ET properties of various high-valent metal-oxo species have merited increasing attention.<sup>5,6</sup> In this context, we have recently reported the first example of binding of metal ions, such as Sc<sup>3+</sup> and Ca<sup>2+</sup>, to a nonheme oxoiron(IV) complex, [(TMC)Fe<sup>IV</sup>(O)]<sup>2+</sup> (TMC = 1,4,8,11-tetramethyl-1,4,8,11-tetraazacyclotetradecane), and the crystal structure of the Sc<sup>3+</sup>-bound [(TMC)Fe<sup>IV</sup>(O)]<sup>2+</sup> complex was determined by X-ray crystallography.<sup>7</sup> The binding of Sc<sup>3+</sup> to [(TMC)Fe<sup>IV</sup>(O)]<sup>2+</sup> resulted in change in the number of electrons transferred from ferrocene (Fc) to the oxoiron complex.<sup>7</sup> However, the ET rate from Fc to [(TMC)Fe<sup>IV</sup>(O)]<sup>2+</sup> was decelerated by the binding of Sc<sup>3+</sup> to [(TMC)Fe<sup>IV</sup>(O)]<sup>2+</sup> because of an increase in the reorganization energy of ET.<sup>7</sup> Although there are many examples for acceleration of ET rates for reduction of organic electron acceptors by metal ions,<sup>8–10</sup> such acceleration effects of metal ions on the reduction of high-valent metal-oxo species have never been reported previously.

We report herein for the first time remarkable acceleration effects of metal ions on rates of ET reduction of [(N4Py)Fe<sup>IV</sup>(O)]<sup>2+</sup> (N4Py = *N,N*-bis(2-pyridylmethyl)-*N*-bis(2-pyridyl)methylamine).<sup>11</sup> Such accelerated ET by metal ions is regarded as metal ion-coupled electron transfer (MCET),<sup>8</sup> in analogy to proton-coupled electron transfer (PCET),<sup>12,13</sup> as shown in Scheme 1. The change in the one-electron reduction potential depending on metal ion concentration is determined by the redox titration in the presence of metal ion. The MCET mechanism is discussed on the basis of the thermodynamics, kinetics, and products obtained in the reactions carried out in the presence of a metal ion.

**Scheme 1.** MCET of [(N4Py)Fe<sup>IV</sup>(O)]<sup>2+</sup>



When [Fe<sup>II</sup>(bpy)<sub>3</sub>]<sup>2+</sup> (bpy = 2,2'-bipyridine) was employed as an electron donor, no ET from [Fe<sup>II</sup>(bpy)<sub>3</sub>]<sup>2+</sup> (*E*<sub>ox</sub> = 1.06 V vs SCE)<sup>14</sup> to [(N4Py)Fe<sup>IV</sup>(O)]<sup>2+</sup> (*E*<sub>red</sub> = 0.51 V) occurred in acetonitrile (MeCN), which is in agreement with the highly positive free energy change of ET ( $\Delta G_{\text{et}} = 0.55$  eV). In the presence of scandium triflate (Sc(CF<sub>3</sub>SO<sub>3</sub>)<sub>3</sub>), however, the ET proceeded efficiently, as shown in Figure 1. As the reaction proceeds, the absorption bands due to

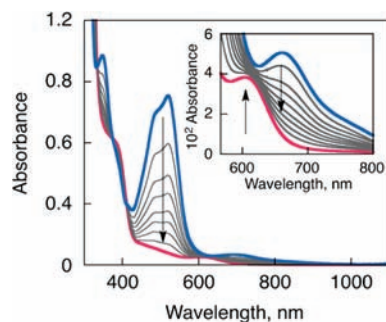


**Figure 1.** Visible spectral change observed in ET from [Fe<sup>II</sup>(bpy)<sub>3</sub>]<sup>2+</sup> (1.1 × 10<sup>-4</sup> M) to [(N4Py)Fe<sup>IV</sup>(O)]<sup>2+</sup> (1.1 × 10<sup>-4</sup> M) in the presence of Sc<sup>3+</sup> (1.0 × 10<sup>-2</sup> M) in MeCN at 298 K.

[Fe<sup>II</sup>(bpy)<sub>3</sub>]<sup>2+</sup> ( $\lambda_{\text{max}} = 520$  nm) and [(N4Py)Fe<sup>IV</sup>(O)]<sup>2+</sup> ( $\lambda_{\text{max}} = 695$  nm) decrease, accompanied by a weak absorption band that remains, due to [Fe<sup>III</sup>(bpy)<sub>3</sub>]<sup>3+</sup> ( $\lambda_{\text{max}} = 600$  nm), and clean isosbestic points (Figure 1).

Formation of [Fe<sup>III</sup>(bpy)<sub>3</sub>]<sup>3+</sup> was also confirmed by EPR measurement. The solution containing [(N4Py)Fe<sup>IV</sup>(O)]<sup>2+</sup> and [Fe<sup>II</sup>(bpy)<sub>3</sub>]<sup>2+</sup> exhibited no EPR signal; however, after addition of 5 equiv of Sc<sup>3+</sup> the solution showed clear EPR signals due to [Fe<sup>III</sup>(bpy)<sub>3</sub>]<sup>3+</sup> (*g* = 2.6 and 1.6) (Figure 2a).<sup>15</sup> The EPR signal at *g* = 4.2 is assigned to an Fe(III) species with an intermediate spin (*S* = 3/2) by comparison with EPR spectra of Fe(III) complexes with *S* = 3/2.<sup>16</sup> Alternatively, a rhombic *S* = 5/2 Fe(III) species may also afford an EPR signal at *g* = 4.2. Further addition of 30 equiv of Sc<sup>3+</sup> resulted in a decrease in the signal at *g* = 4.2,

<sup>†</sup> Osaka University.  
<sup>‡</sup> Ewha Womans University.

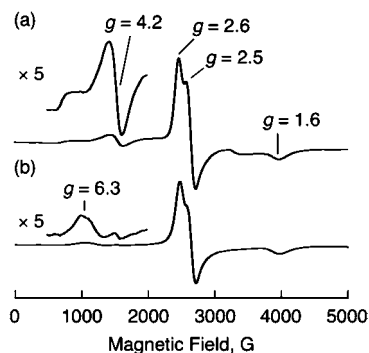


**Figure 2.** (a) EPR spectrum of an MeCN solution containing  $[\text{Fe}^{\text{II}}(\text{bpy})_3]^{2+}$  ( $1.0 \times 10^{-3}$  M),  $[(\text{N4Py})\text{Fe}^{\text{IV}}(\text{O})]^{2+}$  ( $1.0 \times 10^{-3}$  M), and 5 equiv of  $\text{Sc}^{3+}$  ( $5.0 \times 10^{-3}$  M), measured at 77 K. (b) EPR spectrum of an MeCN solution containing  $[\text{Fe}^{\text{II}}(\text{bpy})_3]^{2+}$  ( $1.0 \times 10^{-3}$  M),  $[(\text{N4Py})\text{Fe}^{\text{IV}}(\text{O})]^{2+}$  ( $1.0 \times 10^{-3}$  M), and 30 equiv of  $\text{Sc}^{3+}$  ( $3.0 \times 10^{-2}$  M), measured at 77 K.

accompanied by the appearance of a new signal at  $g = 6.3$ , which may be assigned to an axial  $S = 5/2$  Fe(III) species by comparison with EPR spectra of high-spin Fe(III) complexes (Figure 2b).<sup>17</sup> A similar change in the EPR spectra was observed in ET from octamethylferrocene ( $E_{\text{ox}} = -0.04$  V vs SCE) to  $[(\text{N4Py})\text{Fe}^{\text{IV}}(\text{O})]^{2+}$  (see Supporting Information, Figure S1).<sup>6</sup> The identification of the intermediate and high-spin Fe(III) products depending on concentration of  $\text{Sc}^{3+}$  is discussed together with the thermodynamic and kinetic data (vide infra).

When  $[\text{Fe}^{\text{II}}(\text{bpy})_3]^{2+}$  was replaced by  $[\text{Ru}^{\text{II}}(\text{bpy})_3]^{2+}$  ( $E_{\text{ox}} = 1.24$  V vs SCE),<sup>18</sup> which is a weaker reductant than  $[\text{Fe}^{\text{II}}(\text{bpy})_3]^{2+}$  ( $E_{\text{ox}} = 1.06$  V vs SCE),<sup>14</sup> the ET oxidation by  $[(\text{N4Py})\text{Fe}^{\text{IV}}(\text{O})]^{2+}$  in the presence of  $\text{Sc}^{3+}$  was in equilibrium; the concentration of the remaining  $[\text{Ru}^{\text{II}}(\text{bpy})_3]^{2+}$  decreased with an increase in  $\text{Sc}^{3+}$  concentration, as shown in Figure 3a (see Supporting Information,

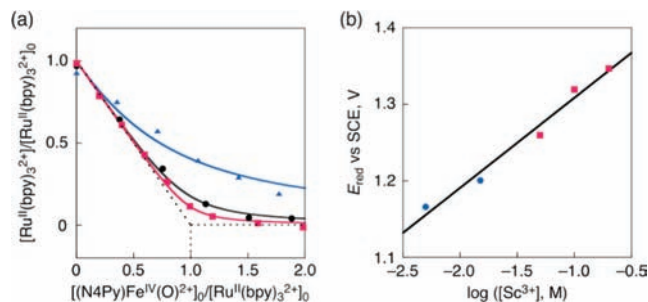
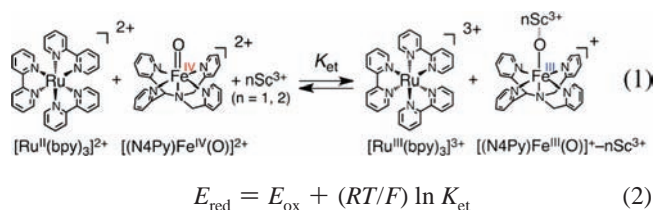


**Figure 3.** (a) Spectroscopic titration at 450 nm for the disappearance of  $[\text{Ru}^{\text{II}}(\text{bpy})_3]^{2+}$  as a function of equiv of  $[(\text{N4Py})\text{Fe}^{\text{IV}}(\text{O})]^{2+}$  added to a solution of  $[\text{Ru}^{\text{II}}(\text{bpy})_3]^{2+}$  and  $\text{Sc}^{3+}$  (red squares, 200 mM; black circles, 100 mM; blue triangles, 50 mM) in MeCN at 298 K. (b)  $[\text{Sc}^{3+}]$  dependence of  $E_{\text{red}}$  of  $[(\text{N4Py})\text{Fe}^{\text{IV}}(\text{O})]^{2+}$  in MeCN at 298 K.  $E_{\text{red}}$  values were derived from equilibrium constants ( $K_{\text{et}}$ ) of the ET from electron donor (blue circles,  $[\text{Ru}^{\text{II}}(\text{Me}_2\text{-bpy})_3]^{2+}$ ; red squares,  $[\text{Ru}^{\text{II}}(\text{bpy})_3]^{2+}$ ) to  $[(\text{N4Py})\text{Fe}^{\text{IV}}(\text{O})]^{2+}$ .

Figure S2, for the visible spectral changes in ET from  $[\text{Ru}^{\text{II}}(\text{bpy})_3]^{2+}$  to  $[(\text{N4Py})\text{Fe}^{\text{IV}}(\text{O})]^{2+}$  in the presence of  $\text{Sc}^{3+}$ ). The ET equilibrium constants ( $K_{\text{et}}$ ) in eq 1 were then determined by global fitting of plots in Figure 3a. The one-electron reduction potentials of  $[(\text{N4Py})\text{Fe}^{\text{IV}}(\text{O})]^{2+}$  ( $E_{\text{red}}$ ) in the presence of different amounts of  $\text{Sc}^{3+}$  were also determined from the  $K_{\text{et}}$  values and the  $E_{\text{ox}}$  value of  $[\text{Ru}^{\text{II}}(\text{bpy})_3]^{2+}$  using the Nernst equation (eq 2). The  $E_{\text{red}}$  values were also determined from the  $K_{\text{et}}$  values obtained from the ET equilibrium between  $[\text{Ru}^{\text{II}}(\text{Me}_2\text{-bpy})_3]^{2+}$  ( $\text{Me}_2\text{-bpy} = 4,4'$ -dimethyl-2,2'-bipyridine) ( $E_{\text{ox}} = 1.13$  V vs SCE)<sup>19</sup> and  $[(\text{N4Py})\text{Fe}^{\text{IV}}(\text{O})]^{2+}$  in the presence of different amounts of  $\text{Sc}^{3+}$  in MeCN at 298 K (see Figure S3 and Table S1 in the Supporting Information for the visible spectral changes in ET from  $[\text{Ru}^{\text{II}}(\text{Me}_2\text{-bpy})_3]^{2+}$  to



$[(\text{N4Py})\text{Fe}^{\text{IV}}(\text{O})]^{2+}$  and the  $K_{\text{et}}$  and  $E_{\text{red}}$  values, respectively).

A plot of  $E_{\text{red}}$  vs  $\log [\text{Sc}^{3+}]$  is shown in Figure 3b, which exhibits a linear correlation with a slope of 118 mV/log  $[\text{Sc}^{3+}]$ . This indicates that the one-electron reduction of  $[(\text{N4Py})\text{Fe}^{\text{IV}}(\text{O})]^{2+}$  is accompanied by binding of two  $\text{Sc}^{3+}$  ions to  $[(\text{N4Py})\text{Fe}^{\text{III}}(\text{O})]^+$  ( $n = 2$  in eq 1), in accordance with the Nernst equation (eq 3),<sup>20</sup> where  $E_{\text{red}}^{\circ}$  is the one-electron reduction potential without  $\text{Sc}^{3+}$ , and  $K_1$  and  $K_2$  are the formation constants of 1:1 and 1:2 complexes of  $[(\text{N4Py})\text{Fe}^{\text{III}}(\text{O})]^+$  with one  $\text{Sc}^{3+}$  and two  $\text{Sc}^{3+}$  ions, respectively. When  $K_1[\text{Sc}^{3+}]$  and  $K_2[\text{Sc}^{3+}] \gg 1$ , the slope of the plot of  $E_{\text{red}}$  vs  $\log [\text{Sc}^{3+}]$  is  $2 \times (2.3RT/F)$ , which corresponds to 118 mV/log  $[\text{Sc}^{3+}]$  at 298 K, in agreement with the result in Figure 3b. The  $E_{\text{red}}$  value in the presence of 0.20 M  $\text{Sc}^{3+}$  is shifted to 1.35 V vs SCE, which is 0.84 V higher than the value in its absence.

$$E_{\text{red}} = E_{\text{red}}^{\circ} + (2.3RT/F) \log(1 + K_1[\text{Sc}^{3+}] + K_1K_2[\text{Sc}^{3+}]^2) \quad (3)$$

Since the Nernst plot in Figure 3b indicates that two  $\text{Sc}^{3+}$  ions bind to  $[(\text{N4Py})\text{Fe}^{\text{III}}(\text{O})]^+$  with large excess of  $\text{Sc}^{3+}$ , the Fe(III) species detected by EPR in Figure 2b may be assigned to a 1:2 complex between  $[(\text{N4Py})\text{Fe}^{\text{III}}(\text{O})]^+$  and  $\text{Sc}^{3+}$  ion,  $[(\text{N4Py})\text{Fe}^{\text{III}}(\text{O})]^+ - (\text{Sc}^{3+})_2$ .<sup>21,22</sup> In such a case, the Fe(III) species in Figure 2a may be assigned to a 1:1 complex between  $[(\text{N4Py})\text{Fe}^{\text{III}}(\text{O})]^+$  and  $\text{Sc}^{3+}$ ,  $[(\text{N4Py})\text{Fe}^{\text{III}}(\text{O})]^+ - \text{Sc}^{3+}$ .<sup>21</sup>

Formation of the 1:2 complex,  $[(\text{N4Py})\text{Fe}^{\text{III}}(\text{O})]^+ - (\text{Sc}^{3+})_2$ , is supported not only by the thermodynamic measurements in Figure 3b but also by the kinetic measurements (vide infra). The ET rate constants from  $[\text{Fe}^{\text{II}}(\text{bpy})_3]^{2+}$  to  $[(\text{N4Py})\text{Fe}^{\text{IV}}(\text{O})]^{2+}$  were determined by monitoring a decrease in absorption peaks at 520 and 695 nm due to  $[\text{Fe}^{\text{II}}(\text{bpy})_3]^{2+}$  and  $[(\text{N4Py})\text{Fe}^{\text{IV}}(\text{O})]^{2+}$ , respectively. Using the same concentration of  $[\text{Fe}^{\text{II}}(\text{bpy})_3]^{2+}$  and  $[(\text{N4Py})\text{Fe}^{\text{IV}}(\text{O})]^{2+}$  in the presence of a large excess of  $\text{Sc}^{3+}$ , the rate obeyed second-order kinetics, and the second-order rate constants ( $k_{\text{obs}}$ ) in the presence of various concentrations of  $\text{Sc}^{3+}$  were determined from the second-order plot (see Supporting Information, Figure S5). The dependence of  $k_{\text{obs}}$  on  $[\text{Sc}^{3+}]$  is shown in Figure 4, where the  $k_{\text{obs}}$  value increases with a first-order dependence on  $[\text{Sc}^{3+}]$  at low concentrations, changing to a second-order dependence at high

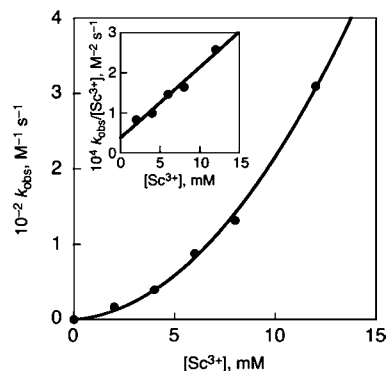


**Figure 4.** Dependence of  $k_{\text{obs}}$  on  $[\text{Sc}^{3+}]$  for the ET from  $[\text{Fe}^{\text{II}}(\text{bpy})_3]^{2+}$  (85  $\mu\text{M}$ ) to  $[(\text{N4Py})\text{Fe}^{\text{IV}}(\text{O})]^{2+}$  (85  $\mu\text{M}$ ) in the presence of  $\text{Sc}^{3+}$  (2.0–12.5 mM) in MeCN at 298 K. Inset: Plot of  $k_{\text{obs}}/[\text{Sc}^{3+}]$  vs  $[\text{Sc}^{3+}]$ .

concentrations, as given by eq 4.<sup>23</sup> The  $k_1$  and  $k_2$  values were determined from the intercept and the slope of the linear plot of  $k_{\text{obs}}/[\text{Sc}^{3+}]$  vs  $[\text{Sc}^{3+}]$  (inset of Figure 4), respectively. The  $k_{\text{obs}}$  value in the presence of 12 mM of  $\text{Sc}^{3+}$  is  $2.5 \times 10^2 \text{ M}^{-1} \text{ s}^{-1}$ , which is ca.  $10^8$ -fold larger than the predicted value without  $\text{Sc}^{3+}$ .<sup>24</sup>

$$k_{\text{obs}} = [\text{Sc}^{3+}](k_1 + k_2[\text{Sc}^{3+}]) \quad (4)$$

When we employed Fc as an electron donor ( $E_{\text{ox}} = 0.37 \text{ V}$ ), ET was accelerated by the addition of not only  $\text{Sc}^{3+}$  but also other metal ions, such as  $\text{Y}^{3+}$ ,  $\text{Lu}^{3+}$ ,  $\text{Zn}^{2+}$ ,  $\text{Mg}^{2+}$ , and  $\text{Ca}^{2+}$ , which are weaker Lewis acids than  $\text{Sc}^{3+}$ . The  $k_1$  and  $k_2$  values for various metal ions were also determined from the dependence of  $k_{\text{obs}}$  on concentrations of metal ions in Figure 5a using eq 5, where  $k_0$  is

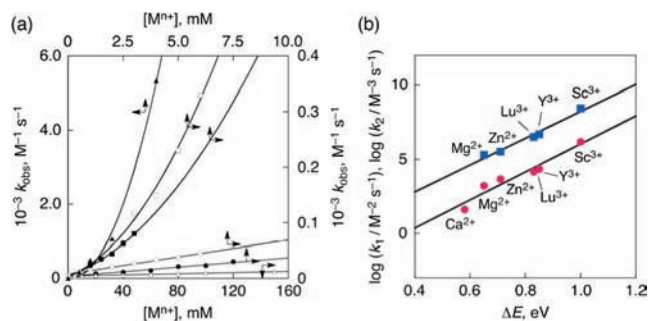


**Figure 5.** (a) Dependence of  $k_{\text{obs}}$  of ET from Fc ( $2.0 \times 10^{-3} \text{ M}$ ) to  $[(\text{N4Py})\text{Fe}^{\text{IV}}(\text{O})]^{2+}$  ( $1.0 \times 10^{-4} \text{ M}$ ) on metal ion concentrations (closed triangles,  $\text{Sc}^{3+}$ ; open squares,  $\text{Y}^{3+}$ ; closed squares,  $\text{Lu}^{3+}$ ; open circles,  $\text{Zn}^{2+}$ ; closed circles,  $\text{Mg}^{2+}$ ; open triangles,  $\text{Ca}^{2+}$ ) in MeCN at 298 K. (b) Plots of  $\log k_1$  (red circles) and  $\log k_2$  (blue squares) vs  $\Delta E$  (quantitative measure of Lewis acidity of metal ions).

the ET rate constant without metal ion (Supporting Information, Figures S6 and S7).

$$k_{\text{obs}} = k_0 + k_1[\text{M}^{n+}] + k_2[\text{M}^{n+}]^2 \quad (5)$$

We have previously reported that the binding energies ( $\Delta E$ ) of metal ions with  $\text{O}_2^-$  can be evaluated from the  $g_{zz}$  values of the  $\text{O}_2^- - \text{M}^{n+}$  complexes and that the  $\Delta E$  values are well correlated with logarithm of rate constants of MCET reduction of *p*-benzoquinone as well as  $\text{O}_2$ .<sup>9</sup> Plots of  $\log k_1$  and  $\log k_2$  vs  $\Delta E$  are shown in Figure 5b, where  $\log k_1$  and  $\log k_2$  are linearly correlated with  $\Delta E$ .<sup>25</sup> Thus, the stronger the Lewis acidity of metal ions, the larger become the rate constants ( $k_1$  and  $k_2$ ) of MCET from Fc to  $[(\text{N4Py})\text{Fe}^{\text{IV}}(\text{O})]^{2+}$ .

In summary, we have demonstrated that metal ions promote ET reduction of  $[(\text{N4Py})\text{Fe}^{\text{IV}}(\text{O})]^{2+}$  markedly. The MCET reactivity increases with increasing the Lewis acidity of metal ions. Among metal ions,  $\text{Sc}^{3+}$  is the most effective, exhibiting  $10^8$ -fold acceleration of the MCET rate.

**Acknowledgment.** This work at Osaka University (S.F.) was supported by a Grant-in-Aid (No. 20108010) and a Global COE program, “the Global Education and Research Center for Bio-Environmental Chemistry”, from the Ministry of Education, Culture, Sports, Science and Technology, Japan. The research at Ewha Womans University was supported by NRF/MEST through CRI

(to W.N.) and GRL (2010-00353) and WCU (R31-2008-000-10010-0) (to S.F. and W.N.).

**Supporting Information Available:** Experimental details, Table S1, and Figure S1–S7. This material is available free of charge via the Internet at <http://pubs.acs.org>.

## References

- (1) (a) Ferreira, K. N.; Iverson, T. M.; Maghlaoui, K.; Barber, J.; Iwata, S. *Science* **2004**, *303*, 1831. (b) Loll, B.; Kern, J.; Saenger, W.; Zouni, A.; Biesiadka, J. *Nature* **2005**, *438*, 1040. (c) McEvoy, J. P.; Brudvig, G. W. *Chem. Rev.* **2006**, *106*, 4455. (d) Sproviero, E. M.; Gascón, J. A.; McEvoy, J. P.; Brudvig, G. W.; Batista, V. S. *J. Am. Chem. Soc.* **2008**, *130*, 3428. (e) Barber, J. *Chem. Soc. Rev.* **2009**, *38*, 185.
- (2) Ferguson-Miller, S.; Babcock, G. T. *Chem. Rev.* **1996**, *96*, 2889.
- (3) Sono, M.; Roach, M. P.; Coulter, E. D.; Dawson, J. H. *Chem. Rev.* **1996**, *96*, 2841.
- (4) Yin, G. *Coord. Chem. Rev.* **2010**, *254*, 1826.
- (5) (a) Pestovsky, O.; Bakac, A. *J. Am. Chem. Soc.* **2003**, *125*, 14714. (b) Comba, P.; Fukuzumi, S.; Kotani, H.; Wunderlich, S. *Angew. Chem., Int. Ed.* **2010**, *49*, 2622. (c) Hirai, Y.; Kojima, T.; Mizutani, Y.; Shiota, Y.; Yoshizawa, K.; Fukuzumi, S. *Angew. Chem., Int. Ed.* **2008**, *47*, 5772.
- (6) (a) Lee, Y.-M.; Kotani, H.; Suenobu, T.; Nam, W.; Fukuzumi, S. *J. Am. Chem. Soc.* **2008**, *130*, 434. (b) Fukuzumi, S.; Kotani, H.; Suenobu, T.; Hong, S.; Lee, Y.-M.; Nam, W. *Chem.—Eur. J.* **2010**, *16*, 354.
- (7) (a) Fukuzumi, S.; Morimoto, Y.; Kotani, H.; Naumov, P.; Lee, Y.-M.; Nam, W. *Nature Chem.* **2010**, *2*, 756. (b) Karlin, K. D. *Nature Chem.* **2010**, *2*, 711.
- (8) (a) Fukuzumi, S. *Prog. Inorg. Chem.* **2009**, *56*, 49. (b) Fukuzumi, S. *Bull. Chem. Soc. Jpn.* **1997**, *70*, 1. (c) Fukuzumi, S.; Ohkubo, K. *Coord. Chem. Rev.* **2010**, *254*, 372.
- (9) Fukuzumi, S.; Ohkubo, K. *Chem.—Eur. J.* **2000**, *6*, 4532.
- (10) For the effect of Lewis acid metal ions on the catalytic oxidation of alkanes by peroxides, see: Yiu, S.-M.; Man, W.-L.; Lau, T.-C. *J. Am. Chem. Soc.* **2008**, *130*, 10821.
- (11) (a) Lubben, M.; Meetsma, A.; Wilkinson, E. C.; Feringa, B.; Que, L., Jr. *Angew. Chem., Int. Ed.* **1995**, *34*, 1512. (b) Kaizer, J.; Klinker, E. J.; Oh, N. Y.; Rohde, J.-U.; Song, W. J.; Stubna, A.; Kim, J.; Münck, E.; Nam, W.; Que, L., Jr. *J. Am. Chem. Soc.* **2004**, *126*, 472.
- (12) (a) Cukier, R. I.; Nocera, D. G. *Annu. Rev. Phys. Chem.* **1998**, *49*, 337. (b) Mayer, J. M. *Annu. Rev. Phys. Chem.* **2004**, *55*, 363.
- (13) (a) Moyer, B. A.; Meyer, T. J. *Inorg. Chem.* **1981**, *20*, 436. (b) Huynh, M. H. V.; Meyer, T. J. *Chem. Rev.* **2007**, *107*, 5004. (c) Concepcion, J. J.; Jurss, J. W.; Brennaman, M. K.; Hoertz, P. G.; Patrocínio, A. O. T.; Iha, N. Y. M.; Templeton, J. L.; Meyer, T. J. *Acc. Chem. Res.* **2009**, *42*, 1954.
- (14) Fukuzumi, S.; Yoshida, Y.; Urano, T.; Suenobu, T.; Imahori, H. *J. Am. Chem. Soc.* **2001**, *123*, 11331.
- (15) For the EPR spectrum due to  $[\text{Fe}^{\text{III}}(\text{bpy})_3]^{3+}$ , see: DeSimone, R. E.; Drago, R. S. *J. Am. Chem. Soc.* **1970**, *92*, 2343.
- (16) (a) Sakai, T.; Ohgo, Y.; Ikeue, T.; Takahashi, M.; Takeda, M.; Nakamura, M. *J. Am. Chem. Soc.* **2003**, *125*, 13028. (b) Kostka, K. L.; Fox, B. G.; Hendrich, M. P.; Collins, T. J.; Rickard, C. E. F.; Wright, L. J.; Münck, E. *J. Am. Chem. Soc.* **1993**, *115*, 6746.
- (17) (a) Hijazi, I.; Roisnel, T.; Even-Hernandez, P.; Geneste, F.; Cador, O.; Guizouarn, T.; Boitrel, B. *Inorg. Chem.* **2010**, *49*, 7536. (b) Rath, S. P.; Olmstead, M. M.; Balch, A. L. *Inorg. Chem.* **2006**, *45*, 6083. (c) Annaraj, J.; Suh, Y.; Seo, M. S.; Kim, S. O.; Nam, W. *Chem. Commun.* **2005**, 4529.
- (18) Fukuzumi, S.; Nakanishi, I.; Tanaka, K.; Suenobu, T.; Tabard, A.; Guillard, R.; Caemelbecke, E. V.; Kadish, K. M. *J. Am. Chem. Soc.* **1999**, *121*, 785.
- (19) Vögtle, F.; Plevovets, M.; Nieger, M.; Azzellini, G. C.; Credi, A.; Cola, L. D.; Marchis, V. D.; Venturi, M.; Balzani, V. *J. Am. Chem. Soc.* **1999**, *121*, 6290.
- (20) For similar Nernst analyses, see: (a) Yuasa, J.; Suenobu, T.; Fukuzumi, S. *J. Am. Chem. Soc.* **2003**, *125*, 12090. (b) Okamoto, K.; Imahori, H.; Fukuzumi, S. *J. Am. Chem. Soc.* **2003**, *125*, 7014.
- (21) The detection of complexes between  $[(\text{N4Py})\text{Fe}^{\text{III}}(\text{O})]^+$  and  $\text{Sc}^{3+}$  with ESI-MS has yet to be successful.
- (22) The optimized structure of  $[(\text{N4Py})\text{Fe}^{\text{III}}(\text{O})]^+ - (\text{Sc}^{3+})_2$  by the DFT calculation is shown in Figure S4 in the Supporting Information.
- (23) Judging from the dependence of  $k_{\text{obs}}$  on  $[\text{Sc}^{3+}]$  in Figure 4, there should be a weak pre-equilibrium binding of  $\text{Sc}^{3+}$  to  $[(\text{N4Py})\text{Fe}^{\text{IV}}(\text{O})]^{2+}$  prior to electron transfer.
- (24) Although no ET from  $[\text{Fe}^{\text{II}}(\text{bpy})_3]^{2+}$  to  $[(\text{N4Py})\text{Fe}^{\text{IV}}(\text{O})]^{2+}$  occurs without  $\text{Sc}^{3+}$  due to the highly positive free energy change of ET ( $\Delta G_{\text{et}}$ ), the rate constant of ET is predicted on the basis of the Marcus theory of ET using the  $\lambda$  value of 2.74 eV and  $\Delta G_{\text{et}}$  value of 0.55 eV; see ref 6a.
- (25) The  $k_2$  value for  $\text{Ca}^{2+}$  was too small to be determined accurately.

JA109056X